

Displaceable and focus-tunable electrowetting optofluidic lens

LEI LI,¹ JIN-HUI WANG,¹ QIONG-HUA WANG,^{2,4} AND SHIN-TSON WU^{3,5}

¹*School of Electronics and Information Engineering, Sichuan University, Chengdu 610065, China*

²*School of Instrumentation Science and Opto-Electronics Engineering, Beihang University, Beijing 100083, China*

³*College of Optics and Photonics, University of Central Florida, Orlando, Florida 32816, USA*

⁴*qionghua@buaa.edu.cn*

⁵*swu@creol.ucf.edu*

Abstract: A conventional optofluidic lens usually has one liquid-liquid (L-L) interface, which can be deformed to achieve variable focal length. Such a single lens cannot be used alone to realize optical zooming because its back focal distance keeps changing. Here, we report a novel displaceable and focus-tunable electrowetting optofluidic lens. In comparison with the conventional optofluidic lens, our new lens has a different working principle and it can function as an optical zoom lens. The L-L interface can be displaced by a voltage. The object distance and image distance can be adjusted by shifting the L-L interface position to achieve the desired magnification, yet the lens can refocus the image by reshaping the L-L interface with another voltage. Under such condition, only one lens is adequate to realize the zooming functionality. To prove the concept, we fabricate an optofluidic lens whose largest displaceable distance is ~ 8.3 mm and the zooming ratio is $\sim 1.31\times$. The proposed optofluidic lens greatly simplifies the zoom lens system. Widespread application of such an adaptive zoom lens is foreseeable.

© 2018 Optical Society of America under the terms of the [OSA Open Access Publishing Agreement](#)

1. Introduction

Adaptive optofluidic lenses whose focal length is dynamically tunable have found widespread applications in imaging, optical communication, and lighting [1–13]. Various types of optofluidic lenses have been developed including those with a large tuning range and high modulation rates. A common feature of the optofluidic lenses is one tunable liquid surface which can be manipulated by various driving methods including electrowetting [2,3], dielectrophoresis [4,5], elastic membrane [6,7], stimuli-responsive hydrogel [8], and many others [9–20]. Although all the conventional optofluidic lenses can vary the focal lengths, they are not suitable to be directly used as zoom lenses because their back focal distances also keep changing. Therefore, to realize zooming as well as correcting aberration, several optofluidic lenslets [21–23] have to be integrated into an optical system, or an optofluidic lens is fabricated with two or more tunable L-L interfaces [24–27]. However, the zooming manipulation is rather complicated because each radius of the optofluidic lenses must be calculated and optimized before applying a suitable voltage. As a result, the optofluidic zoom lens system is relatively bulky, and it is rather complicated to manipulate several lenses or L-L interfaces synergistically to realize zooming. More recently, a multifunctional liquid lens for variable focus and zoom is proposed [28]. It can realize zooming with a single lens using electromagnetic force. However, the displacement of the L-L interface is relatively small and the gravity effect will affect the lens performance when placed in horizontal direction.

In this paper, we propose a new type of optofluidic lens, called displaceable and focus-tunable electrowetting optofluidic lens. It also has one L-L interface, but this interface can be shifted by an applied voltage. Therefore, the object and image distances can be accurately adjusted by the position of the L-L interface to obtain the required magnification. Afterwards, the optofluidic lens will refocus the image by deforming the L-L interface. Thus, one single optofluidic lens can be used as a zoom lens, which makes the system very compact and easy

to operate. We design and fabricate a zoom system using such a displaceable and focus-tunable electrowetting optofluidic lens. In experiment, the largest displaceable distance of the proposed lens is measured to be ~ 8.3 mm and the zoom ratio is $\sim 1.31 \times$. The combination of translational motion and focal length tunability enables a versatile optics for widespread applications.

2. Schematic and principle

The cross-sectional cell structure and the operating mechanism of our optofluidic lens are depicted in Fig. 1. The proposed optofluidic lens consists of an annular chamber and a central chamber, as Fig. 1(a) depicts. The conductive liquid is injected into the bottom of the two chambers. The rest space is filled with silicone oil. Between the two chambers, there are several holes. Thus, the two chambers are connected by liquids to form a closed-loop fluidic system. The proposed optofluidic lens has two actuation electrodes. The upper cylindrical tube is an electrode. When a voltage (U_1) is applied to this electrode, the contact angle of the conductive liquid is changed due to electrowetting effect, which in turn alters the capillary pressure. And the capillary pressure pulls the conductive liquid upward, which pushes the silicone oil down. Thus, the L-L interface descends in the inner tube, as shown in Fig. 1(b). The inner tube is also an electrode. When a voltage (U_2) is applied to this electrode, the shape of the L-L interface is deformed due to electrowetting effect, resulting in a focal length change (Fig. 1(b)). These two voltages are utilized to control the position and the shape of the optofluidic lens. We can control the degree of translational motion and focal length by controlling U_1 and U_2 , respectively. Thus, our lens can function as a zoom lens. As illustrated in Fig. 1(c), the object and image distances are adjusted by shifting the L-L interface position to achieve the desired magnification. Then, the shape of L-L interface can be deformed by the voltage to obtain the required radius and refocus the image on the image plane. Please note that, due to the law of capillary, these two voltages cannot control the position and the shape of the optofluidic lens arbitrarily. The two voltages should be adjusted to make a force balance, which determines the final curvature and position of the proposed lens.

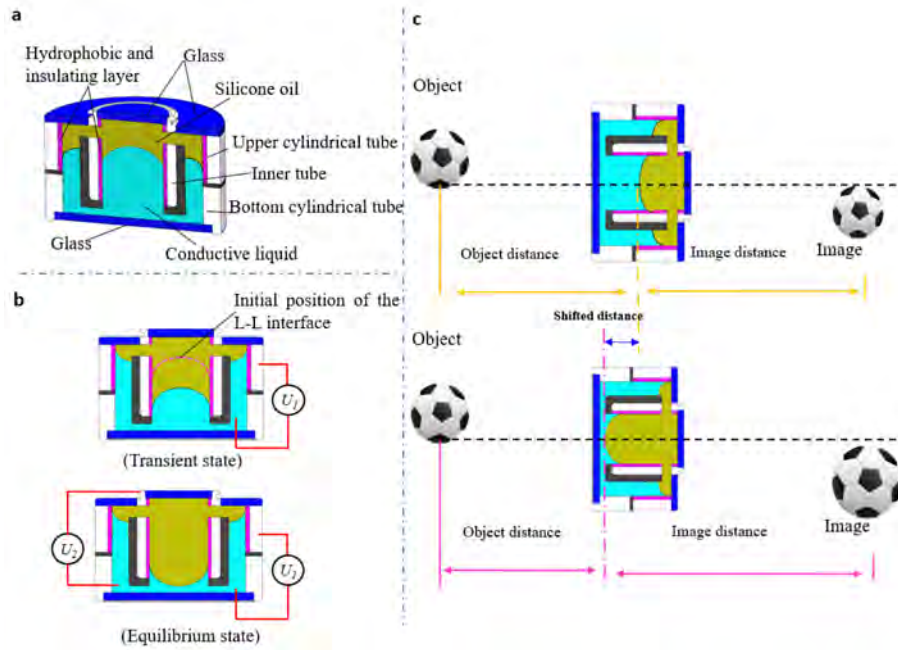


Fig. 1. Schematic cross-sectional structure and operating mechanism of the displaceable and focus-tunable electrowetting optofluidic lens: (a) Cell structure. (b) Moving actuation and deforming actuation. (c) Working principle.

The proposed optofluidic lens is a closed-loop fluidic system, which is based on the law of capillary, as shown in Fig. 2. In an equilibrium state, there is a balance between the applied pressure Δp , the hydrostatic pressure and the effects of surface tension. The Young-Laplace equation [1] becomes

$$\Delta p = \rho gh - \gamma \frac{2}{R}, \quad (1)$$

where h is the liquid height, γ is the surface tension, ρ is the liquid density, R is the mean curvature radius of the tube, and g is the gravitational acceleration. For the initial equilibrium state shown in Fig. 2(a), Eq. (1) can be rewritten as follows:

$$\Delta p_1 = \rho g (H - h_1) - \gamma_{12} \frac{2}{R_1}, \quad (2)$$

$$\Delta p_2 = \rho g (H - h_2) - \gamma_{12} \frac{2}{R_2}, \quad (3)$$

where H is the height of the chamber, γ_{12} is the surface tension of silicon oil/conductive liquid, h_1 is the height of the conductive liquid in the inner tube, h_2 is the height of the conductive liquid in the outer chamber, R_1 is the mean curvature radius of the conductive liquid in the inner tube, and R_2 is the mean curvature radius of the conductive liquid in outer chamber.

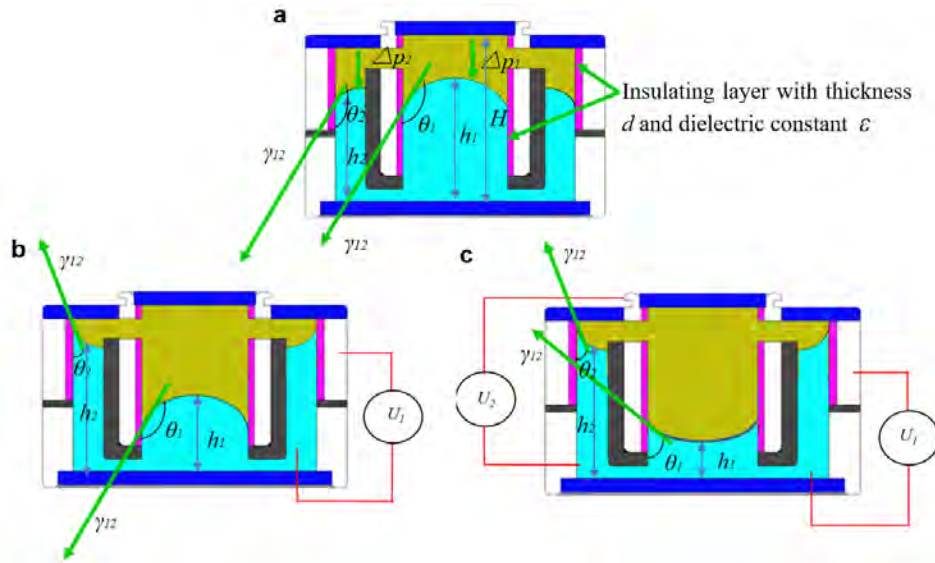


Fig. 2. Analysis of the force balance of the displaceable and focus-tunable electro-wetting optofluidic lens: (a) Initial equilibrium state. (b) Equilibrium state when applying an external voltage U_1 on the device. (c) Equilibrium state when applying an internal voltage U_2 and the external voltage U_1 on the device.

In a closed-loop fluidic system, $\Delta p_1 = \Delta p_2$. Therefore, combining Eqs. (2) and (3) we get

$$\rho g h_1 + \gamma_{12} \frac{2}{R_1} = \rho g h_2 + \gamma_{12} \frac{2}{R_2}, \quad (4)$$

From Eq. (4), we see that the mean curvature radius of the conductive liquid determines the height of the conductive liquid. For our device, we use electro-wetting effect to change the contact angle of the conductive liquid, which results in the change of the curvature radius. Therefore, the height of the conductive liquid is changed.

According to Young–Lippmann equation [2], the relationship of the contact angle θ and the applied voltage U can be described as follows:

$$\cos \theta = \frac{\gamma_1 - \gamma_2}{\gamma_{12}} + \frac{\epsilon}{2\gamma_{12}d} U^2, \quad (5)$$

where ϵ is the dielectric constant of the insulating layer, d is the thickness of the insulating layer, and γ_1 and γ_2 are the interfacial tensions of the hydrophobic layer/silicon oil and hydrophobic layer/conductive liquid, respectively

In an equilibrium state as shown in Fig. 2(b), the voltage U_1 reduces the contact angle θ_1 , which in turn changes R_1 . Therefore, the capillary pressure pulls the conductive liquid upward, leading to the changes of h_1 and h_2 .

For the equilibrium state shown in Fig. 2(c), both voltages U_1 and U_2 reduce the contact angle θ_1 and θ_2 . Thus, R_1 and R_2 are also changed accordingly. The capillary pressures in the inner tube and annular chamber fight against each other and reach a force balance, which determines the final position of the conductive liquid. For this equilibrium state, R_1 should be smaller than R_2 . Thus, the applied voltage U_1 is larger than U_2 .

From above analyses, we can control the applied voltages (U_1 and U_2) to determine the position and the shape of the optofluidic lens and achieve zooming behaviors with a single lens.

3. Operating process

To visually demonstrate the moving and deforming behaviors of the L-L interface, we first fabricated the device using transparent materials. The material of the inner tube and the upper cylindrical tube is polymethyl methacrylate (PMMA). Two flexible conducting films coated with a 3- μm Parylene-C + Teflon layer were inserted into the inner tube and the upper cylindrical tube, respectively. The flexible conducting film is a transparent film coated with a thin indium tin oxide (ITO) layer. Therefore, it is conductive. The film thickness was measured to be 100 μm . The inner tube serves as a deforming actuation electrode, while the upper cylindrical tube serves as a moving actuation electrode. The diameter of the inner tube and the upper cylindrical tube are ~ 6 mm and ~ 16 mm, respectively. Thus, the whole device is transparent. The conductive liquid is NaCl solution, and its density is ~ 1.09 g/cm³ (refractive index $n_1 = 1.35$). To observe the behavior of the L-L interface clearly, we dyed the conductive liquid with a blue pigment. The density of the silicon oil is ~ 1.09 g/cm³ (refractive index $n_2 = 1.50$). A CCD camera was placed on the lateral side of the device. It was used to record the position change of the L-L interface during actuation. Figure 3(a) shows the recorded data when different voltages were applied to the device. The driving voltage of the device is ~ 30 V. Below 30 V, the L-L interface keeps still. When a voltage larger than 30 V is applied, say 40 V, the contact angle of the blue liquid in the annular chamber is changed due to electrowetting effect, which alters the capillary pressure and pulls the liquid flows upward. Thus, the L-L interface in the central chamber moves downward. The shifting distance in the vertical direction was measured to be ~ 2 mm. As the driving voltage increases, the liquid in the annular chamber is lifted up higher so that the shifting distance of the L-L interface gets larger. As the voltage keeps increasing to $U = 50$ V, 60 V, and 80 V, the translational distance increases to ~ 4 mm, ~ 6 mm, and ~ 7 mm, respectively. When $U > 90$ V, the shifting distance remains nearly the same, because the contact angle of the conductive liquid in the annular chamber is saturated, as shown in Fig. 3(b). The largest shifting distance was measured to be ~ 8.3 mm. After we remove the voltage, the surface tension restores the L-L interface to its initial position. A dynamic response video of the moving behavior is also included ([Visualization 1](#)).

To show the behavior of shape deforming, we do a second experiment, as shown in Figs. 3(c) and 3(d). Different from the first experiment, we dye the conductive liquid red. Firstly, we apply a voltage to the annular chamber to generate liquid flow, so that the L-L interface descends. To adjust the L-L interface in the center of the inner tube, we apply a voltage of $U_M = 50$ V. From Fig. 3(c), the L-L interface moves downwards. After 5 seconds, the L-L interface settles in the center of the tube. Then, we apply a voltage (U_D) on the electrode in the inner tube and the shape of the L-L interface starts to deform. The shape gradually deforms from a convex shape to a plane, as shown in Fig. 3(c). In this way, the focal length as well as the position is changed. By accurately controlling the position and shape, the proposed lens can realize a zoom lens. We also measure the optical power of the lens at different voltages, as shown in Fig. 3(d). The shortest focal lengths of the convex and concave shapes are measured to be ~ 66.7 mm and ~ 29.5 mm, respectively. A dynamic response video of the combination of moving and deforming actuation process is also included ([Visualization 2](#)). From the experiment, we can conclude that by only applying two voltages, both the position and the shape of the L-L interface can be accurately adjusted, which confirms the feasibility of the proposed moving adjustment and focusing adjustment method of our lens and makes the one-lens zoom system become feasible.

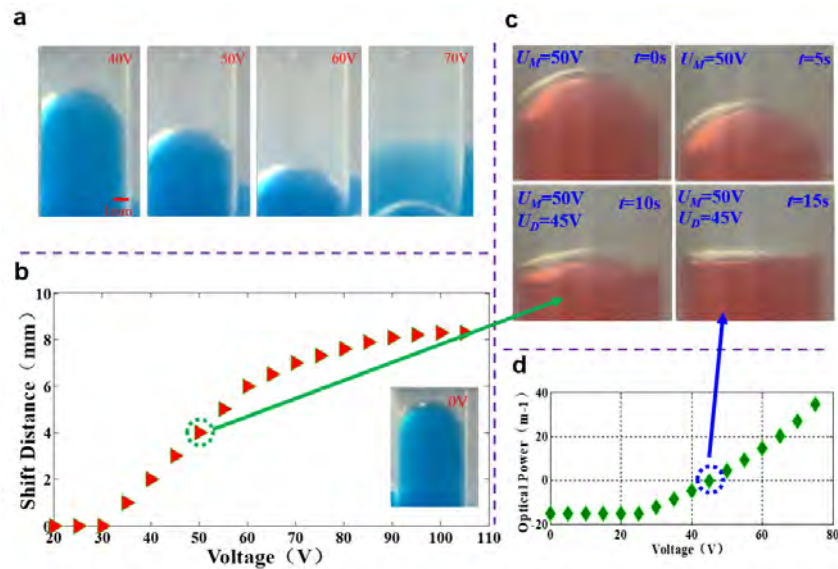


Fig. 3. Performance of moving and deforming actuation of the displaceable and focus-tunable electrowetting optofluidic lens. (a) Moving performance of the proposed lens at different voltages. Blue water is the dyed conductive liquid (see Visualization 1). (b) Moving distance with different voltages. (c) Deforming performance of the proposed lens. U_M is the voltage which is applied for moving actuation. U_D is the voltage which is applied for deforming actuation (see Visualization 2). (d) Optical power with different voltages.

4. Device fabrication

To evaluate the imaging quality, we fabricate a prototype of the optofluidic lens which can be easily integrated into a lens system. The prototype consists of 8 elements, as shown in Fig. 4(a). The inner tube, upper cylindrical tube and bottom cylindrical tube are made of aluminum which serves as the electrode of the device. The inwall of the inner tube and upper cylindrical tube are coated with Teflon as the hydrophobic and insulating layer. The thickness of the coated Parylene-C + Teflon is $\sim 3\mu\text{m}$. The inner tube is drilled with 6 holes to keep the annular chamber and the central cylindrical chamber connected. The inner diameter of the upper cylindrical tube and bottom cylindrical tube is $\sim 16\text{mm}$. The height and inner diameter of the inner tube are $\sim 10.5\text{mm}$ and $\sim 6\text{mm}$, respectively. The insulation layer tube and insulation ring are made of polyfluortetraethylene. The material of the top and bottom window glass is BK7 in glass data of SHOTT [29]. The diameters of the top and bottom window glass are $\sim 8\text{mm}$ and $\sim 18\text{mm}$, respectively. The transparent ring is made of PMMA. The inner and outer diameters are $\sim 10\text{mm}$ and $\sim 20\text{mm}$, respectively. All the elements are stuck together to form the prototype using UV 331 glue, as shown in Fig. 4(b). The size of the whole device is designed to be 20mm (diameter) \times 14.5mm (height).

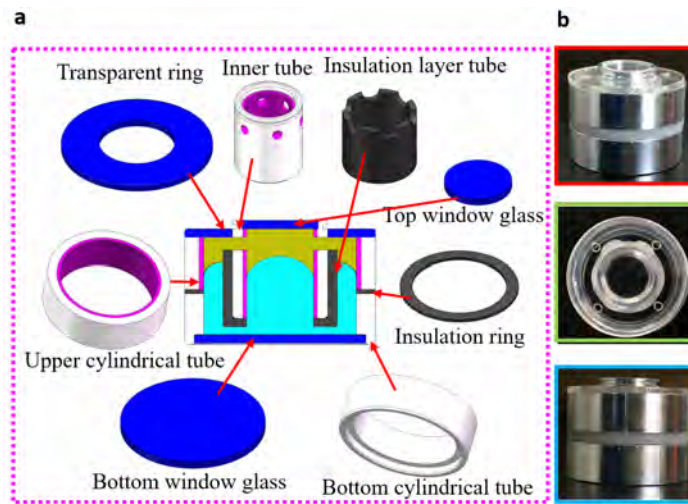


Fig. 4. Fabricated prototype of the displaceable and focus-tunable electrostatic optofluidic lens. (a) All the elements of the device. The inner tube has 6 holes which connects the two chambers. (b) Assembled prototype.

5. Application in zoom system

We assemble an optofluidic zoom system using the fabricated prototype to test the imaging quality and zooming ability. The optofluidic zoom system consists of a displaceable and focus-tunable electrostatic optofluidic lens, a solid lens and a CMOS, as shown in Fig. 5(a).

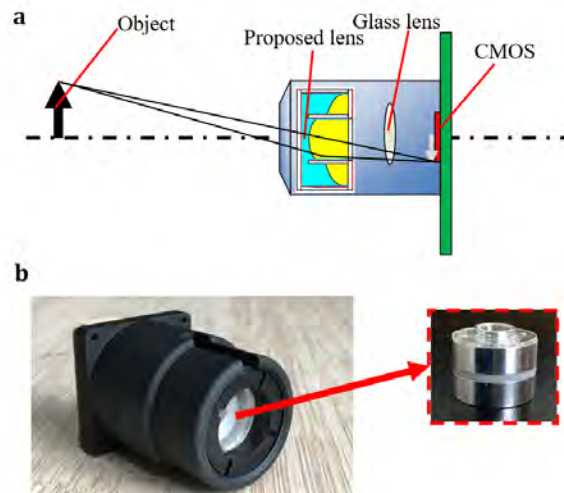


Fig. 5. Optofluidic zoom system using a displaceable and focus-tunable electrostatic optofluidic lens. (a) Setup of the zoom system which consists of a displaceable and focus-tunable electrostatic optofluidic lens and a glass lens. (b) Assembled prototype.

The displaceable and focus-tunable electrostatic optofluidic lens is the crucial part to realize zooming by moving and deforming actuation. The glass lens is used to undertake part of the focal power of the lens system to shorten the back focal distance, since the power of the displaceable and focus-tunable electrostatic optofluidic lens is limited. The CMOS is the image plane. The resolution of the CMOS is 2592×1944 . In the experiment, the object distance is ~ 100 mm. The assembled optofluidic zoom system is shown in Fig. 5(b). Different from conventional optofluidic zoom system, our system has only one tunable lens. Thus, the

system is compact, and the manipulation is very simple. The dimension of the optofluidic zoom system is 30 mm (diameter) \times 45 mm (height).

We performed a real experiment based on the simulation results. The object distance is ~ 100 mm. In the initial state, the object can be imaged on the CMOS, but the image is blurring because of defocusing. As the voltage on the inner tube electrode gradually increases, the L-L interface is deformed, and the image gradually becomes clear, as shown in Fig. 6(b). In this state, the applied voltage is ~ 56 V. Next, we applied a voltage to the upper frame electrode and the L-L interface began to move in the tube. In experiment, we applied ~ 100 V voltage on the upper frame electrode. The shifting distance is ~ 8.3 mm. As a result, the magnification changes significantly, but the image remains blurred. For the conventional optofluidic lens, it is impossible to compensate the changed back focal length. However, for the proposed optofluidic lens, we can gradually adjust the applied voltage on the inner tube to reshape the L-L interface. Finally, a magnified yet sharp image appears at the CMOS. In this condition, the applied voltage is ~ 62 V. Comparing the two states, the image is magnified by $\sim 1.31 \times$. We also measured the magnification versus the applied voltage, and results are plotted in Fig. 7. All the points on the plot are at a given magnification where best focus is found. The magnification increases with the moving voltage, because the image distance increases with the moving voltage. The deforming voltage variation is relatively small, which is within 2.5 V. In this experiment, we see that the magnification is mainly determined by the translational motion of the L-L interface, and the deforming of the L-L interface plays a key role to refocus the image onto the CMOS. The experimental results agree well with the Zemax simulation, which confirms the feasibility of an optical zooming system with a single lens. The proposed novel lens opens a new door for developing compact optical zooming system.

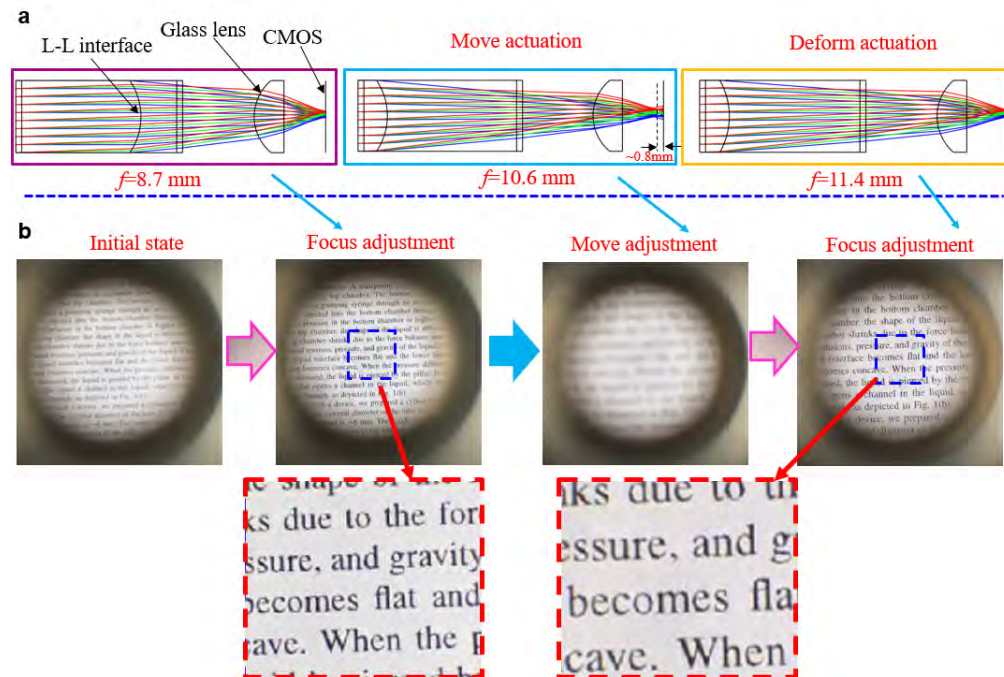


Fig. 6. Imaging experiment using one displaceable and focus-tunable electro-wetting optofluidic lens. (a) Zemax model of the zoom lens system. Firstly, the L-L interface remains in the initial position and deforms the shape to focus image on the CMOS. Then, the position is shifted forward. Finally, the shape of the L-L interface is deformed to refocus the image on the CMOS. (b) Experimental results of zoom in and out state of the proposed optofluidic zoom lens system.

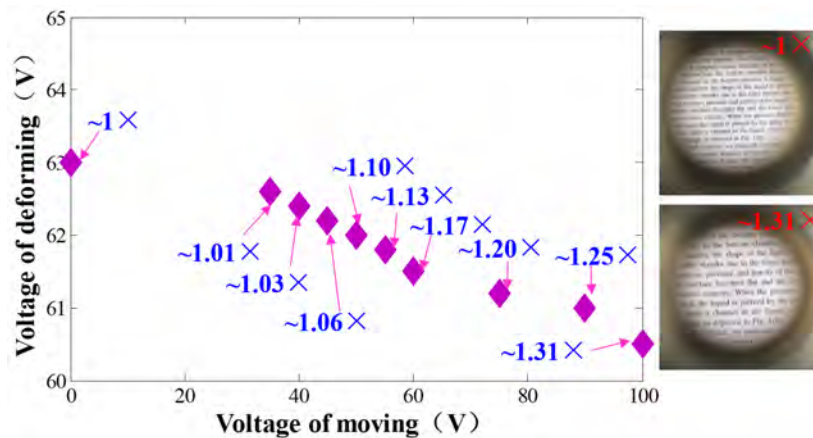


Fig. 7. Applied voltage dependent magnification of the proposed optofluidic lens.

In comparison with the conventional optofluidic lens, our optofluidic lens has a different working principle. A relatively large magnification is achievable by moving the L-L interface, while sharp focus is obtained by reshaping the L-L interface. Such a unique feature is unparalleled by a single conventional optofluidic lens. To realize optical zooming as well as correcting aberration with conventional optofluidic lens, several lenses must be combined together to form a compound lens. However, the zooming manipulation is rather complex because each radius of the optofluidic lenses must be calculated before applying a suitable voltage.

6. Conclusion

We have demonstrated a displaceable and focus-tunable electrowetting liquid lens. Different from the conventional optofluidic lenses, our proposed optofluidic lens has a different working principle and it functions as a zoom lens. The L-L interface can be moved by a voltage to obtain the required magnification, yet the optofluidic lens can refocus the image by deforming the L-L interface. It takes only one such lens to realize both functions. In the experiment, the largest displaceable distance is ~ 8.3 mm and the zoom ratio is $\sim 1.31 \times$. It can make the zoom lens system very compact and easy to integrate. Its potential applications in imaging system, near-eye displays, and consumer electronics are foreseeable.

Funding

National Key R&D Program of China under Grant No. 2017YFB1002900 and the NSFC under Grant Nos. 61505127, 61320106015 and 61535007.

References

1. R. Finn, "Capillary Surface Interfaces," *Not. Am. Math. Soc.* **46**(7), 770–781 (1999).
2. B. Berge, J. Peseux, "Variable focal lens controlled by an external voltage: An application of electrowetting," *Eur. Phys. J. E* **3**(2), 159–163 (2000).
3. S. Kuiper and B. H. W. Hendriks, "Variable-focus liquid lens for miniature cameras," *Appl. Phys. Lett.* **85**(7), 1128–1130 (2004).
4. C. C. Cheng and J. A. Yeh, "Dielectrically actuated liquid lens," *Opt. Express* **15**(12), 7140–7145 (2007).
5. H. Ren, H. Xianyu, S. Xu, and S. T. Wu, "Adaptive dielectric liquid lens," *Opt. Express* **16**(19), 14954–14960 (2008).
6. H. Ren and S. T. Wu, "Variable-focus liquid lens," *Opt. Express* **15**(10), 5931–5936 (2007).
7. D. Y. Zhang, V. Lien, Y. Berdichevsky, J. Choi, and Y. H. Lo, "Fluidic adaptive lens with high focal length tunability," *Appl. Phys. Lett.* **82**(19), 3171–3172 (2003).
8. L. Dong, A. K. Agarwal, D. J. Beebe, and H. Jiang, "Adaptive liquid microlenses activated by stimuli-responsive hydrogels," *Nature* **442**(7102), 551–554 (2006).
9. S. Xu, H. Ren, and S. T. Wu, "Adaptive liquid lens actuated by liquid crystal pistons," *Opt. Express* **20**(27), 28518–28523 (2012).

10. H. Ren, Y. H. Fan, S. Gauza, and S. T. Wu, "Tunable-focus flat liquid crystal spherical lens," *Appl. Phys. Lett.* **84**(23), 4789–4791 (2004).
11. C. A. López and A. H. Hirs, "Fast focusing using a pinned-contact oscillating liquid lens," *Nat. Photonics* **2**(10), 610–613 (2008).
12. D. Koyama, R. Isago, and K. Nakamura, "Compact, high-speed variable-focus liquid lens using acoustic radiation force," *Opt. Express* **18**(24), 25158–25169 (2010).
13. Y. H. Lin, M. S. Chen, and H. C. Lin, "An electrically tunable optical zoom system using two composite liquid crystal lenses with a large zoom ratio," *Opt. Express* **19**(5), 4714–4721 (2011).
14. O. Pishnyak, S. Sato, and O. D. Lavrentovich, "Electrically tunable lens based on a dual-frequency nematic liquid crystal," *Appl. Opt.* **45**(19), 4576–4582 (2006).
15. Z. Wang, M. Lei, B. Yao, Y. Cai, Y. Liang, Y. Yang, X. Yang, H. Li, and D. Xiong, "Compact multi-band fluorescent microscope with an electrically tunable lens for autofocusing," *Biomed. Opt. Express* **6**(11), 4353–4364 (2015).
16. Y. Nakai, M. Ozeki, T. Hiraiwa, R. Tanimoto, A. Funahashi, N. Hiroi, A. Taniguchi, S. Nonaka, V. Boilot, R. Shrestha, J. Clark, N. Tamura, V. M. Draviam, and H. Oku, "High-speed microscopy with an electrically tunable lens to image the dynamics of in vivo molecular complexes," *Rev. Sci. Instrum.* **86**(1), 013707 (2015).
17. K. Mishra, C. Murade, B. Carreel, I. Roghair, J. M. Oh, G. Manukyan, D. van den Ende, and F. Mugele, "Optofluidic lens with tunable focal length and asphericity," *Sci. Rep.* **4**(1), 6378 (2015).
18. D. Zhu, C. Li, X. Zeng, and H. Jiang, "Tunable-focus microlens arrays on curved surfaces," *Appl. Phys. Lett.* **96**(8), 081111 (2010).
19. C. A. López, C. C. Lee, and A. H. Hirs, "Electrochemically activated adaptive liquid lens," *Appl. Phys. Lett.* **87**(13), 134102 (2005).
20. S. Xu, H. Ren, and S. T. Wu, "Dielectrophoretically tunable optofluidic devices," *J. Phys. D Appl. Phys.* **46**(48), 483001 (2013).
21. S. Lee, M. Choi, E. Lee, K. D. Jung, J. H. Chang, and W. Kim, "Zoom lens design using liquid lens for laparoscope," *Opt. Express* **21**(2), 1751–1761 (2013).
22. L. Li, D. Wang, C. Liu, and Q. H. Wang, "Zoom microscope objective using electrowetting lenses," *Opt. Express* **24**(3), 2931–2940 (2016).
23. L. Li, D. Wang, C. Liu, and Q. H. Wang, "Ultrathin zoom telescopic objective," *Opt. Express* **24**(16), 18674–18684 (2016).
24. L. Li and Q. H. Wang, "Zoom lens design using liquid lenses for achromatic and spherical aberration corrected target," *Opt. Eng.* **51**(4), 043001 (2012).
25. D. Kopp, T. Brender, and H. Zappe, "All-liquid dual-lens optofluidic zoom system," *Appl. Opt.* **56**(13), 3758–3763 (2017).
26. H. Choi and Y. Won, "Fluidic lens of floating oil using round-pot chamber based on electrowetting," *Opt. Lett.* **38**(13), 2197–2199 (2013).
27. P. Waibel, D. Mader, P. Liebetaut, H. Zappe, and A. Seifert, "Chromatic aberration control for tunable all-silicone membrane microlenses," *Opt. Express* **19**(19), 18584–18592 (2011).
28. I. S. Park, Y. Park, S. H. Oh, J. W. Yang, and S. K. Chung, "Multifunctional liquid lens for variable focus and zoom," *Sens. Actuator A-Phys.* **273**, 317–323 (2018).
29. SCHOTT, http://www.schott.com/optocs_devices/english/download/